fractal and fractional

MDPI

Article

Simplified Relation Model of Soil Saturation Permeability Coefficient and Air-Entry Value and Its Application

Gaoliang Tao [1,2], Zhijia Wu [1], Wentao Li [1,*], Yi Li [1] and Heming Dong [3]

[1] School of Civil Engineering, Architecture and Environment, Hubei University of Technology, Wuhan 430068, China; tgl1979@126.com (G.T.); wzj2301214319@163.com (Z.W.); yi.li10566@outlook.com (Y.L.)
[2] School of Intelligent Construction, Wuchang University of Technology, Wuhan 430223, China
[3] Shiyan City Transportation Investment Co., Ltd., Shiyan 442000, China; dhm.wayne@hotmail.com
* Correspondence: wli20201027@hbut.edu.cn

Abstract: Based on the Tao and Kong (TK) model and the fractal model of the soil–water characteristic curve, a simplified model of the relationship between the saturated permeability coefficient and the air-entry value is established in this study: $k_s = k_0 \psi_a{}^{-2}$. It is shown that the saturated permeability coefficient of soil is determined by its maximum pore size. In order to facilitate the mutual prediction of saturation permeability coefficient and air-entry value, based on the data of five types of soil in the UNSODA database, the comprehensive proportionality constant k_0 of the five types of soil were obtained: sand $k_0 = 0.03051$; clay $k_0 = 0.001878$; loam $k_0 = 0.001426$; sandy loam $k_0 = 0.009301$; and silty clay loam $k_0 = 0.0007055$. Based on the obtained comprehensive proportionality constant k_0 and the relationship model between saturated permeability coefficient and air intake value, the air-entry value of five kinds of soils in the existing literature and the SoilVision database were calculated. Comparing the calculated air-entry value with the measured one, the results showed that the model simplifies the traditional air-entry value prediction method to some extent and can effectively predict the air-entry value of different types of soil. On the whole, the model better predicts the air-entry value for sandy, clay, and silty clay loam than loam and sandy loam.

Keywords: model; saturated permeability coefficient; air-entry value; maximum pore; comprehensive proportionality constant

Citation: Tao, G.; Wu, Z.; Li, W.; Li, Y.; Dong, H. Simplified Relation Model of Soil Saturation Permeability Coefficient and Air-Entry Value and Its Application. *Fractal Fract.* **2021**, *5*, 180. https://doi.org/10.3390/fractalfract5040180

Academic Editor: Norbert Herencsar

Received: 1 September 2021
Accepted: 18 October 2021
Published: 23 October 2021

1. Introduction

Soil in nature is a kind of three-phase material, so it is of great significance to study the related characteristics of soil in depth for engineering construction, environmental protection, and energy mining. As a way to describe soil characteristics, a soil–water characteristic curve (SWCC) contains an enormous amount of basic soil information. The soil–water characteristic curve characterizes the relationship between water content (including mass water content w, volume water content θ_w, saturation Sr, and water content e_w) and suction in the soil (mainly referring to the matrix suction, which reflects the influence and effect of the boundary surface). The soil–water characteristic curve can reflect the water-holding capacity of the soil and the size and distribution of pores in the soil. Research on the shear strength, consolidation theory, and permeability theory of unsaturated soil involves its application by measuring the balance state of soil samples. The soil–water characteristic curve can be drawn with the water content and corresponding suction. The SWCC is usually divided into the boundary effect zone, the transition zone, and the residual zone according to the degree of saturation of soil. Soils change from the saturated state to the unsaturated state corresponding to the change from the boundary effect zone to the transition zone. Usually, these two zones are differentiated by their air-entry values. Therefore, as an important parameter of the SWCC, the air-entry value has a significant effect on soil shear strength, deformation, permeability, and even the interaction mechanism between water, air, and soil particles within the soil. The air-entry value is a critical point on the

soil–water characteristic curve, which means that the largest pores in the soil can hardly resist the applied suction and cause water loss. At this time, the applied matrix suction is the air-entry value.

Many researchers in the world have made outstanding contributions to the study of air-entry value. Bouwer [1] conducted field measurements of soil air-entry values with a cylindrical lid permeameter equipped with a riser and a vacuum gauge, and they established a step function to explore hydraulic conductivity. Fredlund and Xing [2] proposed a fitting formula for the measured SWCC and obtained the air-entry value of the soil by plotting and solving the fitted SWCC. Fallow and Elrick [3] externally added a tension bottle to the permeameter and measured the air-entry value of the soil on site, thereby providing an improved description of the hydraulic properties of soils. Nemati et al. [4] proposed a method for measuring the air-entry value in a rapid tension chamber. Different potting substrates were in contact with unsaturated bodies located outside the tension chamber, and the potential in the cabin was detected to calculate the air-entry values of peat substrates. Sakaki et al. [5] found that there was a close relationship between the diameter of the characteristic particle and the air-entry value. The results showed that the average pore size had a dominant effect on the air-entry value. Based on this, a simple air-entry value prediction was proposed. Chui et al. [6] analyzed two geological cases in Singapore, and they used the ordinary leather method and the simple Kriging method (SK) to estimate the spatial variability of the air-entry value of the soil. Ni et al. [7] used the instantaneous profile method to quantify the influence of plant roots on the air-entry value, and they found that the presence of roots significantly increased the air-entry value of silt. Under mixed planting with rotted roots, the vegetation soil showed a significant decrease in the air-entry value. Slowik et al. [8] proposed an air-entry value identification method through regarding the air-entry value as an indicator of the early cracking of materials. Soltani et al. [9] investigated the relationship between air-entry value and adaptive parameters by establishing an explicit equation method based on the air-entry value and residual state suction. Wijaya et al. [10] obtained the shrinkage curves of multiple soil samples, and their results showed that the minimum void ratio of the shrinkage curve has a significant effect on the air-entry value.

At present, the air-entry value is usually determined by using the SWCC. However, the measurement of the SWCC requires experimental instruments. The SWCC can be measured by a variety of methods and materials, including a pressure plate test, a vacuum dryer, the cooling mirror dew point method, filter paper, the unsaturation test, and an unsaturated triaxial apparatus [11–18]. The method used to test the soil–water characteristic curve usually provides a series of discrete data points between the matrix suction and water content. However, to use the soil–water characteristic curve to study the phenomena of the permeability, stress, and deformation of unsaturated soil, one needs complete curves and continuous mathematical formulas. At the same time, direct test measurement is often time-consuming and labor-intensive, with harsh conditions, and the measured test data are insufficient. Therefore, it is necessary and meaningful to use the soil–water characteristic curve model for data fitting and prediction. These limitations are mainly manifested in expensive equipment and operation difficulty. In the absence of experimental equipment, it is difficult for people to measure the air-entry value of soil, which can be more quickly and effectively obtained via indirect prediction. Therefore, the authors of this study combined the SWCC fractal model with the existing permeability model and further established a model of constant of proportionality for the permeability coefficient. This model was found to simplify the traditional air-entry value prediction method and overcome the limitations of practical measurement methods. The applicability and effectiveness of the model were verified by using the relevant data of existing soil.

2. Establishment of Prediction Model

The prediction model of the saturated permeability coefficient can be obtained from the Tao and Kong (TK) model [19], namely Formula (1):

$$k_s = k_c \int_{\theta_r}^{\theta_s} \frac{dx}{\psi^2(x)} \tag{1}$$

where k_s is the saturated permeability coefficient, θ_s is the saturated volumetric water content, θ_r is the residual volumetric water content, and ψ is the matrix suction.

In Formula (1):

$$k_c = \frac{\gamma {T_S}^2 \cos^2 \alpha}{2 p_i \mu} \tag{2}$$

where γ is the unit weight of water, μ is the absolute viscosity of water, T_s is the table surface tension, α is the contact angle, and p_i is the ratio of the actual length of the i-th pore channel to the length of the soil sample. For the same type of soil, k_c is a constant.

According to the fractal model of the soil–water characteristic curve proposed in the literature [20], the volumetric water content can be expressed as follows:

$$\begin{cases} \theta = \frac{e_0}{1+e_0} - 1 + \left(\frac{\psi_a}{\psi}\right)^{3-D} & \psi \geq \psi_a \\ \theta = \theta_s = \frac{e_0}{1+e_0} & \psi < \psi_a \end{cases} \tag{3}$$

where e_0 is the void ratio, ψ_a is the air-entry value; D is the fractal dimension, and θ_s is the volumetric water content.

Differentiate Formula (3):

$$dx = d\theta = (D-3){\psi_a}^{3-D} \psi^{D-4} d\psi \tag{4}$$

Substitute Formula (4) into Formula (1):

$$k_s = k_c (D-3) \int_{\psi_d}^{\psi_a} {\psi_a}^{3-D} \psi^{D-6} d\psi \tag{5}$$

After calculation and simple transformation, Formula (6) can be obtained:

$$k_s = k_c \frac{D-3}{D-5} {\psi_a}^{-2} \left[1 - \left(\frac{\psi_d}{\psi_a}\right)^{D-5}\right] \tag{6}$$

where $\psi_a \ll \psi_d$, $D-5 < -2$.

Formula (6) can be simplified to Formula (7):

$$k_s = \frac{D-3}{D-5} k_c {\psi_a}^{-2} \tag{7}$$

It can be seen from Formula (7) that the saturated permeability coefficient of the soil and the square of the air-entry value have an inverse proportional relationship. According to the literature [19,21], the clay content of natural soil has a direct relationship with the fractal dimension D as follows.

The clay content is within a certain range for the same type of soil. The corresponding fractal dimension does not vary much, and compared to the square of the air-entry value, the fractal dimension has a negligible effect on permeability [19,21]. In order to simplify the calculation, the authors of this article set the part containing the fractal dimension D and the permeability coefficient proportional constant k_c as a constant. This constant is named the comprehensive proportionality constant k_0. Then, Formula (7) is transformed into:

$$k_s = k_0 {\psi_a}^{-2} \tag{8}$$

According to the law of the capillary, the air-entry value is inversely proportional to the maximum pore diameter of the soil, so Formula (8) shows that the saturated permeability coefficient is directly proportional to the maximum pore diameter. This indicates that the saturated permeability coefficient of the soil is essentially controlled by the maximum pore diameter.

3. Determine Constant of Proportionality k_0 for the Model

3.1. Source of Experimental Data

The main sources of the database collection in this study were the soil-related data in the UNSODA database [22]. The five soil types in this database are sand, clay, loam, sandy loam, and silty clay loam. The database only contains data on the SWCC, without the air-entry value.

The authors of a previous study [23] obtained the relationship between the air-entry value and the basic parameters in the VG model, which is presented as follows:

$$\alpha = \left(\frac{0.76}{\psi_a}\right)^{1.26} \tag{9}$$

where α is the fitting parameter of the model and ψ_a is the air-entry value of the soil.

In this paper, the VG model was firstly used to fit the volumetric water content and suction of the soil in the UNSODA database to obtain the standard SWCC and the corresponding fitting parameters. Then, the corresponding air-entry value was calculated by Formula (9).

The VG model equation is given by Formula (10):

$$\theta_w = \theta_r + \frac{\theta_s - \theta_r}{\left[1 + (\alpha\psi)^n\right]^m} \tag{10}$$

where θ_w is the volumetric water content; θ_r is the residual water content; θ_s is the saturated water content; ψ is the matrix suction; and α, m, and n are the fitting parameters of the model, usually $m = 1 - 1/n$.

The data obtained from the database are summarized in Table 1, and Figure 1 shows the results of statistical data processing and box diagram plotting.

Table 1. Basic statistical data obtained from the UNSODA database.

Type of Soil	Sample	Mean Value		Standard Deviation	
		AEV (kPa)	k_s (cm/s)	*AEV* (kPa)	k_s (cm/s)
Sand	50	2.23	0.024	1.41	0.051
Clay	47	2.51	0.0053	5.21	0.0092
Loam	38	2.94	0.0007	2.39	0.0008
Sandy loam	43	4.44	0.0009	2.99	0.0011
Silty clay loam	40	6.12	0.000024	1.79	0.000011

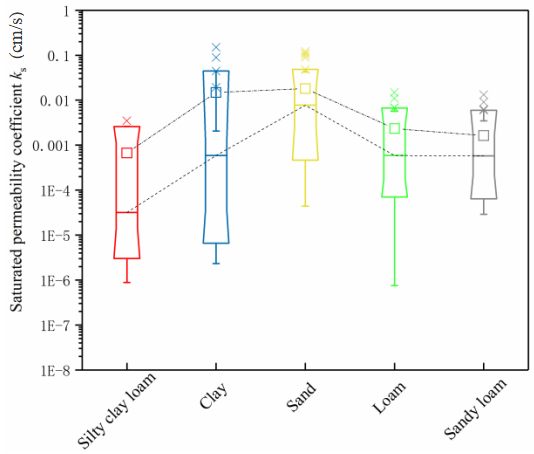

(**a**)

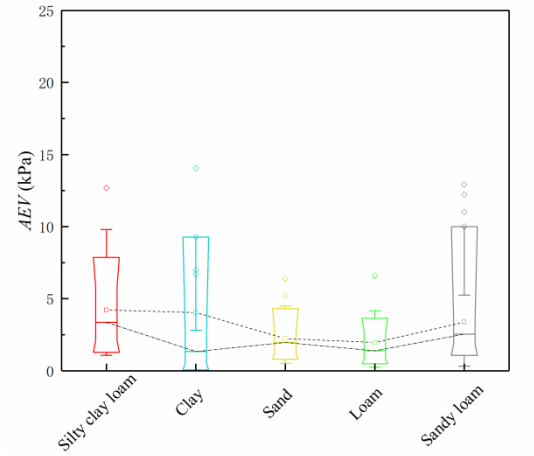

(**b**)

Figure 1. (**a**) Saturated permeability coefficient for various soils; (**b**) air-entry values for various soils.

3.2. Determination of the Comprehensive Proportionality Constant

Formula (8) was used to fit the data to obtain an image with ${\psi_a}^{-2}$ as the horizontal axis and k_s as the vertical axis. The collected soil data were plotted into a scatter plot and then linearly fitted. The linear function with the highest correlation coefficient was selected as the fitting result. The slope of the linear function was taken as the comprehensive constant of proportionality. The fitting result is shown in Figure 2, and the comprehensive constants of proportionality of the five soils are shown in Table 2.

Table 2. The comprehensive proportional constants of proportionality of the five soils obtained by fitting.

Type of Soil	Comprehensive Proportionality Constant k_0	Fitted Correlation Coefficient R^2
Sand	0.03051	0.9158
Clay	0.001878	0.8797
Loam	0.001426	0.8373
Sandy loam	0.009301	0.9067
Silty clay loam	0.0007055	0.8267

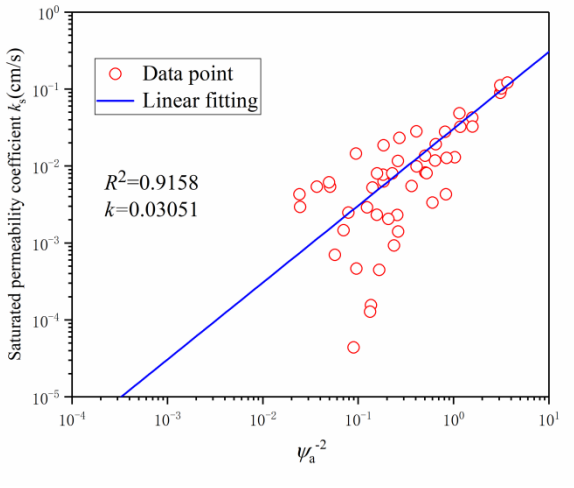

(**a**)

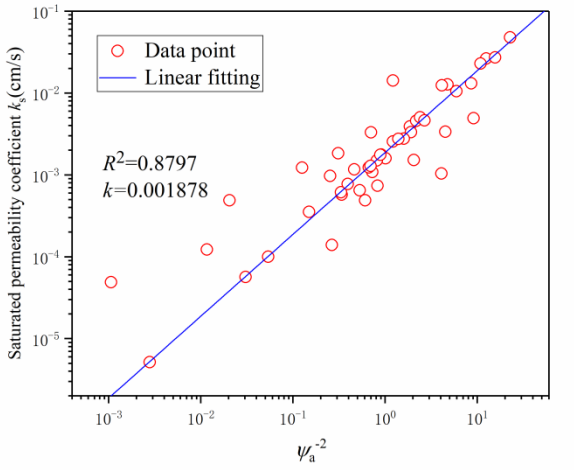

(**b**)

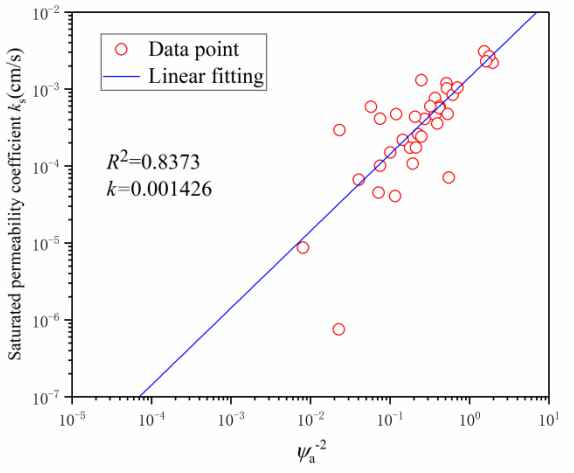

(**c**)

Figure 2. *Cont*.

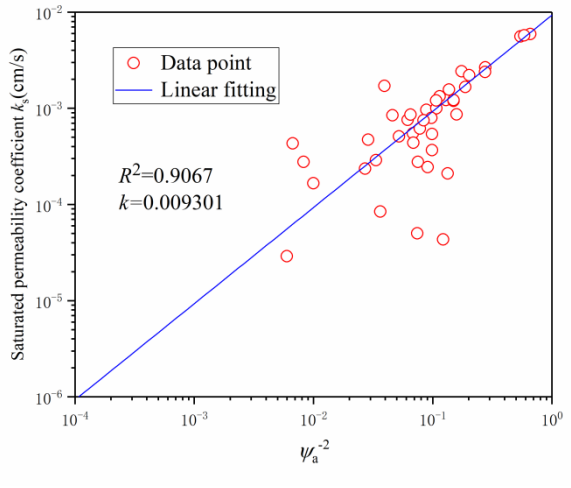

(**d**)

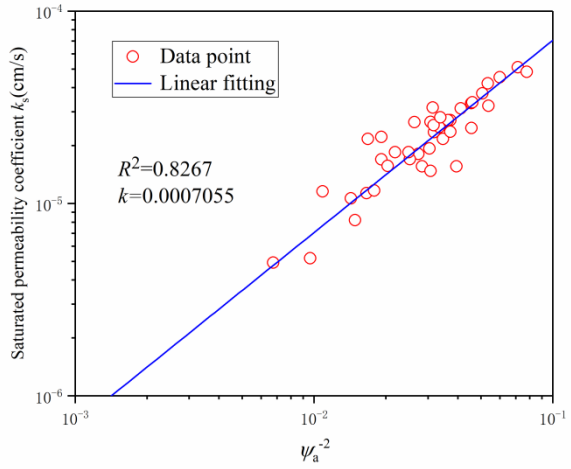

(**e**)

Figure 2. Comprehensive constant of proportionality of (**a**) sand, (**b**) clay, (**c**) loam, (**d**) sandy loam, and (**e**) silty clay loam.

In the process of solving the comprehensive proportionality constant, the correlation between sand and sandy loam was found to be over 0.9 when fitting the relevant data and within 0.8–0.9 among the other three soils.

4. Model Verification and Discussion

4.1. Data Verification

In order to verify the accuracy of the obtained comprehensive proportionality constant and the rationality of this method, the authors of this paper used a simplified relationship model between the saturated permeability coefficient and air-entry value of soil and the comprehensive proportionality constant k_0 determined above to calculate the corresponding air-entry value through the saturated permeability coefficient; then, they conducted a comparative analysis with the measured values. The validated soil data came from the clay and SoilVision database in [24] for sand, loam, sandy loam, and silty clay loam.

(i). Experimental data of Hunan clay

Part of the verification data came from the literature [24]. In this paper, the SWC-150 Fredlund SWCC instrument produced by the American Soilmoisture Company was used for the pressure plate test, and SWCC data of Hunan red clay with different initial dry

densities were obtained. Falling head permeability tests were performed to obtain the saturated permeability coefficients of Hunan red clay with different initial dry densities.

The soil–water characteristic curve obtained by fitting the measured scatter diagram of the soil–water characteristic curve with the VG model is shown in Figure 3. The corresponding air-entry value was obtained using the tangent line graphing method. Specifically, the tangent line was plotted through the inflection point on the curve. There was an intersection point between the tangent line and the initial volumetric water content (vertical axis). The abscissa of the intersection point was taken as the air-entry value. We obtained the inflection point by taking the second-order derivation of lg(ψ) and setting the result of the second-order derivation equal to zero. The coordinates of the inflection point are shown in Figure 3. For different initial dry densities of 1.3, 1.35, 1.4, 1.45, 1.5, and 1.6 g/cm^3, the air-entry values were 2.65, 4.33, 6.70, 8.25, 9.77, and 13.42 kPa, respectively.

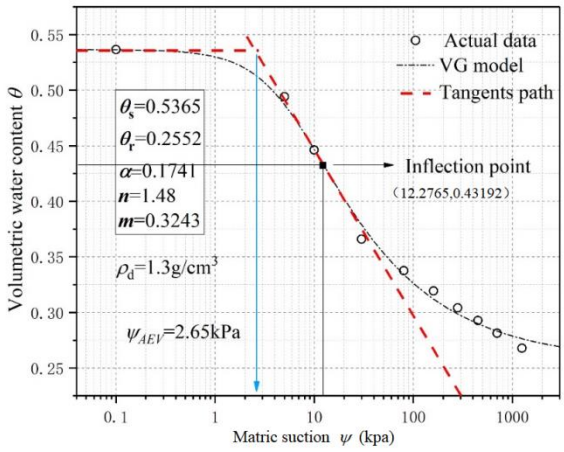

(**a**)

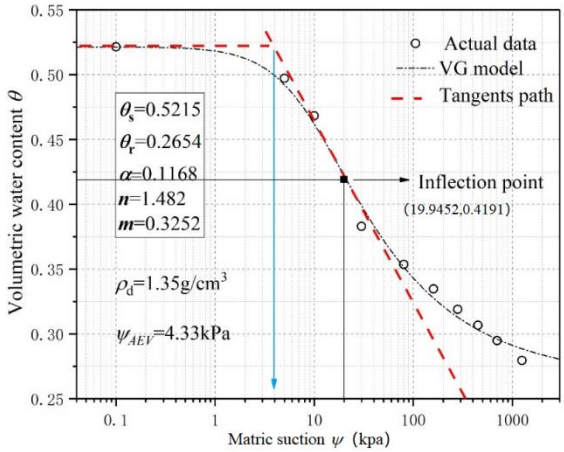

(**b**)

Figure 3. *Cont.*

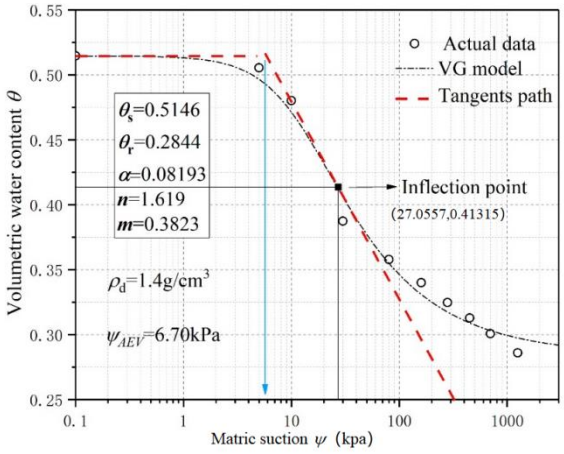

(**c**)

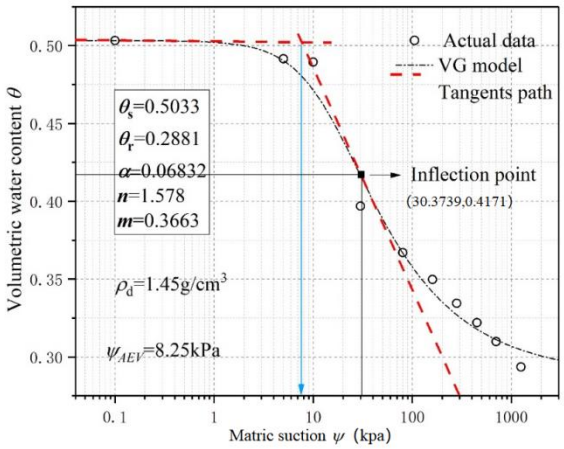

(**d**)

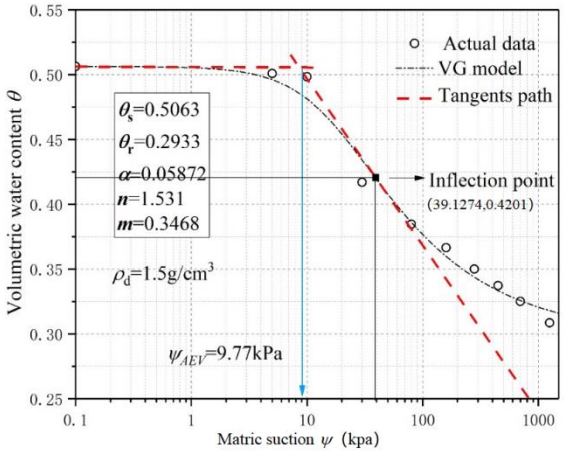

(**e**)

Figure 3. *Cont*.

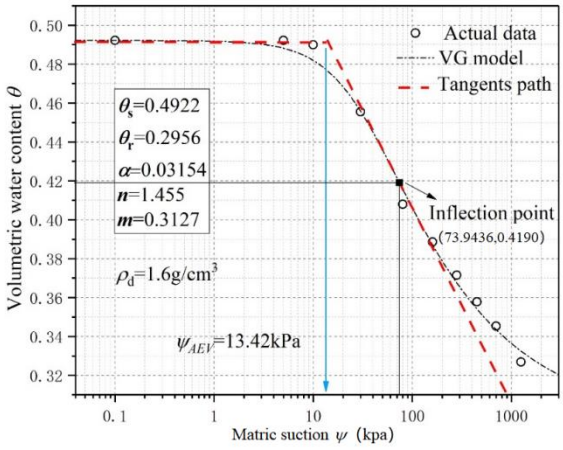

(**f**)

Figure 3. Soil–water characteristic curve and air-entry value of Hunan clay with different initial dry densities: (**a**) 1.3 g/cm^3, (**b**) 1.35 g/cm^3, (**c**) 1.4 g/cm^3, (**d**) 1.45 g/cm^3, (**e**) 1.5 g/cm^3, and (**f**) 1.6 g/cm^3.

(ii). SoilVision Database

The soil data in the SoilVision database include the saturated permeability coefficient, the standard soil–water characteristic curve, and the air-entry value of the soil [25]. The authors of this paper selected the relevant data of four soils in the database: sand, loam, sandy loam, and silt clay loam. Multiple samples were selected for each type of soil, and these samples were numbered, as shown in Tables 3–7.

Table 3. Basic sand information.

The Serial Number of the Figure	The Serial Number of the Database	Saturated Permeability Coefficient k_s (cm/s)	AEV in the Database (kPa)	Predicted AEV (kPa)
1	4283	0.0133	1.36	1.51
2	4346	0.020083	1.56	1.23
3	4417	0.010944	1.64	1.66
4	4461	0.0089444	1.64	1.84
5	4986	0.021167	0.84	1.19
6	3906	0.013417	2.28	1.50
7	5136	0.00875	2.9	1.86
8	4247	0.0040278	2.34	2.74
9	4333	0.00825	1.14	1.91
10	4498	0.0048889	2.81	2.48

Table 4. Basic clay information.

The Serial Number of the Figure	Dry Density (g/cm^3)	Saturated Permeability Coefficient k_s (cm/s)	AEV Obtained by Drawing (kPa)	Predicted AEV (kPa)
1	1.3	7.72×10^{-4}	2.65	1.56
2	1.35	4.15×10^{-4}	4.33	2.13
3	1.4	2.49×10^{-4}	6.7	2.75
4	1.45	1.73×10^{-4}	8.25	3.29
5	1.5	4.78×10^{-5}	9.77	6.27
6	1.6	9.92×10^{-6}	13.42	13.76

Table 5. Basic loam information.

The Serial Number of the Figure	The Serial Number of the Database	Saturated Permeability Coefficient k_s (cm/s)	AEV in the Database (kPa)	Predicted AEV (kPa)
1	1451	8.3333×10^{-5}	8.94	4.14
2	4407	4.860×10^{-3}	0.56	0.54
3	4274	2.7778×10^{-5}	10.49	7.16
4	4273	5.5556×10^{-5}	4.72	5.07
5	4401	2.7778×10^{-5}	3.65	7.16
6	4790	1.8333×10^{-5}	6.2	2.79
7	1441	2.2222×10^{-5}	5.37	8.01
8	1426	5.5556×10^{-6}	14.39	16.02
9	1402	4.1667×10^{-5}	8.62	5.85
10	4409	4.8889×10^{-3}	2.81	2.48

Table 6. Basic sandy loam information.

The Serial Number of the Figure	The Serial Number of the Database	Saturated Permeability Coefficient k_s (cm/s)	AEV in the Database (kPa)	Predicted AEV (kPa)
1	4991	2.50×10^{-4}	2.59	6.10
2	5099	5.56×10^{-5}	8.33	12.94
3	3955	3.53×10^{-4}	3.57	5.13
4	3199	8.33×10^{-5}	6.38	10.56
5	5238	8.19×10^{-4}	1.12	3.37
6	5184	9.72×10^{-4}	3.1	3.09
7	4384	2.92×10^{-2}	0.48	0.56
8	4429	2.39×10^{-4}	3.02	6.24
9	4284	3.61×10^{-4}	2.63	5.08
10	5238	8.19×10^{-4}	1.12	3.37

Table 7. Basic silty clay loam information.

The Serial Number of the Figure	The Serial Number of the Database	Saturated Permeability Coefficient k_s (cm/s)	AEV in the Database (kPa)	Predicted AEV (kPa)
1	4919	7.95×10^{-3}	0.34	0.30
2	4930	6.29×10^{-3}	0.56	0.33
3	4850	2.00×10^{-3}	0.31	0.59
4	4867	5.14×10^{-4}	1.08	1.17
5	4923	7.08×10^{-3}	0.34	0.32
6	4906	4.20×10^{-3}	0.37	0.41
7	4916	5.04×10^{-3}	0.35	0.37
8	4845	8.29×10^{-3}	0.29	0.29
9	4779	2.78×10^{-5}	8.67	5.04
10	4910	4.02×10^{-3}	0.65	0.42
11	4908	1.27×10^{-2}	0.37	0.24
12	4913	9.59×10^{-3}	0.25	0.27
13	4912	2.47×10^{-2}	0.35	0.17

4.2. Model Verification

Based on the values of k_0 determined in Section 3, (sand k_0 = 0.03051; clay k_0 = 0.001878; loam k_0 = 0.001426; sandy loam k_0 = 0.009301; and silty clay loam k_0 = 0.0007055), the saturated permeability coefficients of multiple soil samples were used in Formula (8) to

obtain predicted soil air-entry values. A comparison of the measured and predicted results of the four types of soils is shown in Figure 4. The specific calculated and measured values are shown in Tables 3–7.

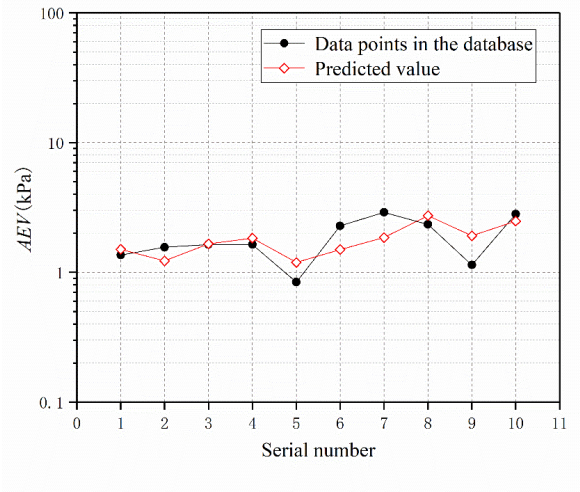

(**a**)

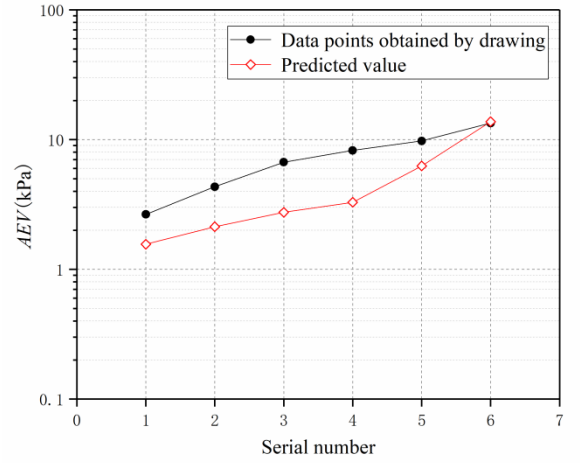

(**b**)

Figure 4. *Cont*.

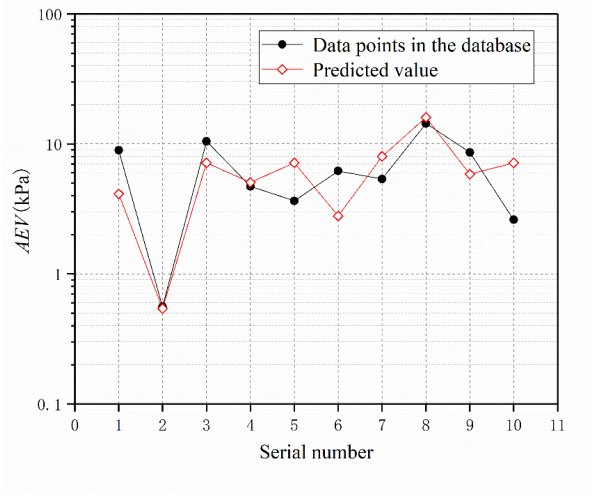

(**c**)

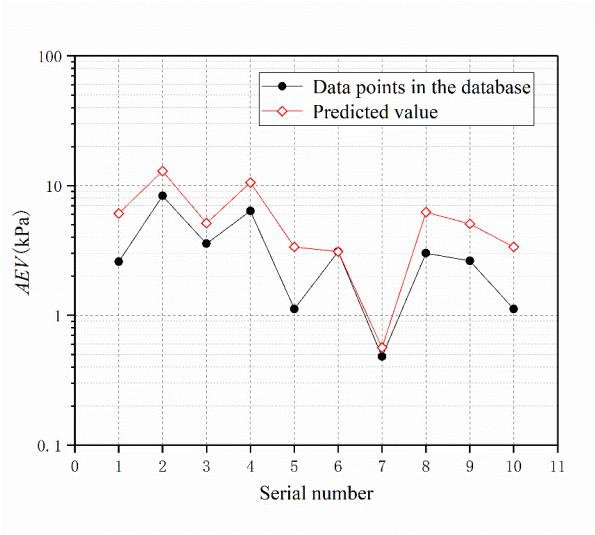

(**d**)

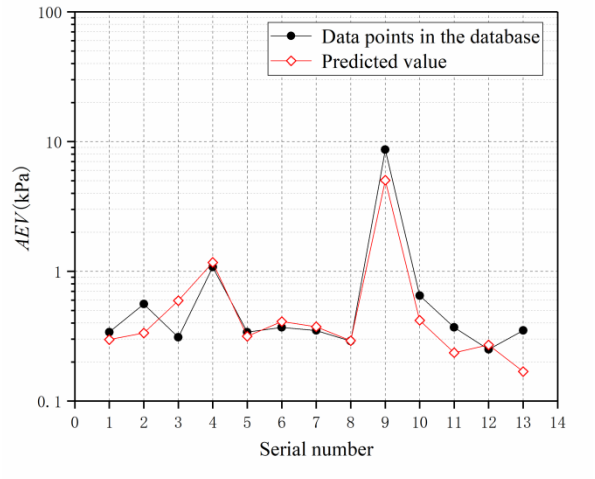

(**e**)

Figure 4. Measured and predicted values of air-entry values of various soils: (**a**) sand, (**b**) clay, (**c**) loam, (**d**) sandy loam, and (**e**) silty clay loam.

It can be seen from Figure 4 that the model could better predict the air-entry value of sand. Specifically, there were five measured data points that were close to the predicted points. Hunan clay was used as a verified clay soil sample, and its predicted values under different initial dry densities were close to the measured values. When the dry densities were 1.5 and 1.6 g/cm^3, the measured values were in good agreement with the predicted values. When the dry density was less than 1.5 g/cm^3, the predicted value was lower than the measured value. Overall, the predicted value was close to the measured value. The model predicted the air-entry value worse for loam and sandy loam than clay and sand. The predictions for loam and sandy loam soils were overall lower than those for clay and sandy soils. Of the selected data points, only three and two in the loam and sandy loam soils, respectively, were close to the measured values. The predicted and measured values of the silt clay loam soil were in the same order of magnitude, and there were six data points that were in good agreement with the predicted values.

4.3. Discussion

The above mentioned theoretical calculations and related experimental verification results showed that the prediction model is applicable to predict air-entry values to a certain extent. The prediction model was based on fractal theory and the TK model, and a new prediction model was obtained through the combination of the two theories. Taking sand as an example, the fractal dimension D of sand was found to be roughly in the range of 2.317~2.493 [25]. The reciprocal $\psi_a{}^{-2}$ of the square of the air-entry value of sand was found to vary in the range of 0.1–1. The change of fractal dimension relative to the square of the air-entry value was found to have a negligible effect on the permeability coefficient. According to capillary theory, the reciprocal of the square of the air-entry value is the square of the maximum pore size, indicating that the saturated permeability coefficient is determined by the maximum pore size.

The introduction of the comprehensive proportionality constant k_0 of the permeability coefficient significantly reduces the calculation work of the air-entry value. In this study, the k_0 of different soils could be approximated as a constant, which facilitated the mutual prediction between the air-entry value and the saturated permeability coefficient. That is to say, once the type of soil was determined, the saturated permeability coefficient could be used to predict the air-entry value, and vice versa.

For the determination of the comprehensive proportionality constant, the selection of data could have certain limitations. The fitting correlation of some soil data is relatively high. It is not easy to select the right amount of data and obtain fitting results with high correlations. For common soil types, the verification in this study generally presented good results, which could facilitate the establishment of this simplified model. For other soil types, the applicability of this simplified model needs to further verification. In this study, we collected a total of 218 sets of data, which was not enough to verify all soil types. More experimental data need to be considered in future research.

5. Conclusions

In this study, a simplified relationship model between the saturated permeability coefficient and the air-entry value for five types of soil was investigated, and a large amount of experimental data were collected to determine the model proportionality constant k_0. The air intake values of different types of soils were separately predicted by using the simplified relationship model of the saturation permeability coefficient of the soil, the air intake value proposed in this paper, and the determined proportionality constant k_0. A comparative analysis was carried out with the available experimental data. The main conclusions are as follows:

(1) The relationship model between the saturated permeability coefficient and air-entry value was determined to be $k_s = k_0 \psi_a{}^{-2}$, where k_0 is the comprehensive proportional constant.

(2) The comprehensive constant of proportionality k_0 of the five soils was determined as follows: sand k_0 = 0.03051; clay k_0 = 0.001878; loam k_0 = 0.001426; sandy loam k_0 = 0.009301; and silty clay loam k_0 = 0.0007055.
(3) The model better predicted the air-entry value for sand, clay, and silty clay loam compared to loam and sandy loam.
(4) The model in this study can be used to make mutual predictions of the saturation permeability coefficient and air-entry value. Limited data on soil types were used to validate the model, so more experimental data need to be considered in future research.

Author Contributions: G.T. and Z.W. mostly contributed to the design of the manuscript. Y.L. carried out data collection and processing. W.L. and H.D. were involved in the statistical analysis. W.L. revised the paper. All authors have read and agreed to the published version of the manuscript.

Funding: The work in this paper was supported by grants from Natural Science Foundation of China (No.51978249) and the Innovation Group Project of Hubei Science and Technology Department (No. 2020CFA046), China.

Institutional Review Board Statement: Not applicable.

Informed Consent Statement: Not applicable.

Data Availability Statement: All data, models, and codes generated or used in the research process were obtained through experiments and calculation formulas in the text.

Conflicts of Interest: The authors declare no conflict of interest.

Notation

The following symbols are used in this paper:

k_s the saturated permeability coefficient
θ_s the saturated volumetric water content
θ_r the residual volumetric water content
ψ the matrix suction
γ the unit weight of water
μ the absolute viscosity of water
T_s the table surface tension
α the contact angle
p_i the ratio of the actual length of the i-th pore channel to the length of the soil sample
k_c a constant for the same type of soil
e_0 the void ratio
ψ_a the air-entry value
D the fractal dimension

References

1. Bouwer, H. Rapid field measurement of air entry value and hydraulic conductivity of soil as significant parameters in flow system analysis. *Water Resour. Res.* **1966**, *2*, 729–738. [CrossRef]
2. Fredlund, D.G.; Xing, A. Equations for the soil-water characteristic curve. *Can. Geotech. J.* **1994**, *31*, 521–532. [CrossRef]
3. Fallow, D.; Elrick, D. Field measurement of air-entry and water-entry soil water pressure heads. *Soil Sci. Soc. Am. J.* **1996**, *60*, 1036–1039. [CrossRef]
4. Nemati, M.; Caron, J.; Banton, O.; Tardif, P. Determining air entry value in peat substrates. *Soil Sci. Soc. Am. J.* **2002**, *66*, 367–373. [CrossRef]
5. Sakaki, T.; Komatsu, M.; Takahashi, M. Rules-of-Thumb for Predicting Air-Entry Value of Disturbed Sands from Particle Size. *Soil Sci. Soc. Am. J.* **2014**, *78*, 454–464. [CrossRef]
6. Ip, C.Y.S.; Rahardjo, H.; Satyanaga, A. Spatial variations of air-entry value for residual soils in Singapore. *Catena* **2019**, *174*, 259–268. [CrossRef]
7. Ni, J.; Leung, A.K.; Ng, C.W. Unsaturated hydraulic properties of vegetated soil under single and mixed planting conditions. *Géotechnique* **2019**, *69*, 554–559. [CrossRef]
8. Slowik, V.; Schmidt, M.; Fritzsch, R. Capillary pressure in fresh cement-based materials and identification of the air entry value. *Cem. Concr. Compos.* **2008**, *30*, 557–565. [CrossRef]

9. Soltani, A.; Azimi, M.; Deng, A.; Taheri, A. A simplified method for determination of the soil–water characteristic curve variables. *Int. J. Geotech. Eng.* **2019**, *13*, 316–325. [CrossRef]
10. Wijaya, M.; Leong, E.C.; Rahardjo, H. Effect of shrinkage on air-entry value of soils. *Soils Found.* **2015**, *55*, 166–180. [CrossRef]
11. Khanzode, R.; Vanapalli, S.; Fredlund, D. Measurement of soil-water characteristic curves for fine-grained soils using a small-scale centrifuge. *Can. Geotech. J.* **2002**, *39*, 1209–1217. [CrossRef]
12. Li, J.; Lu, Z.; Guo, L.; Zhang, L.M. Experimental study on soil-water characteristic curve for silty clay with desiccation cracks. *Eng. Geol.* **2017**, *218*, 70–76. [CrossRef]
13. Lu, N.; Wayllace, A.; Carrera, J.; Likos, W.J. Constant flow method for concurrently measuring soil-water characteristic curve and hydraulic conductivity function. *Geotech. Test. J.* **2006**, *29*, 230–241. [CrossRef]
14. Manahiloh, K.N.; Meehan, C.L. Determining the soil water characteristic curve and interfacial contact angle from microstructural analysis of X-ray CT images. *J. Geotech. Geoenviron. Eng.* **2017**, *143*, 04017034. [CrossRef]
15. Nishiumura, T.; Koseki, J.; Fredlund, D.G.; Rahardjo, H. Microporous membrane technology for measurement of soil-water characteristic curve. *Geotech. Test. J.* **2012**, *35*, 201–208. [CrossRef]
16. Peranić, J.; Arbanas, Ž.; Cuomo, S.; Maček, M. Soil-water characteristic curve of residual soil from a flysch rock mass. *Geofluids* **2018**, *2018*, 6297819. [CrossRef]
17. Sahin, H.; Gu, F.; Lytton, R.L. Development of soil-water characteristic curve for flexible base materials using the methylene blue test. *J. Mater. Civ. Eng.* **2015**, *27*, 04014175. [CrossRef]
18. Wang, X.; Benson, C.H. Leak-free pressure plate extractor for measuring the soil water characteristic curve. *Geotech. Test. J.* **2004**, *27*, 163–172. [CrossRef]
19. Tao, G.; Kong, L. A model for determining the permeability coefficient of saturated and unsaturated soils based on micro pore channel and its application. *J. Hydraul. Eng.* **2017**, *48*, 702–709. (In Chinese) [CrossRef]
20. Tao, G.; Kong, L.; Xiao, H.; Ma, Q.; Zhu, Z. Fractal characteristics and fitting analysis of soil–water characteristic curves. *Rock Soil Mech.* **2014**, *35*, 2443–2447. (In Chinese) [CrossRef]
21. Li, D.; Zhang, T. Fractal features of particle size distribution of soils in China. *Soil Environ. Sci.* **2000**, *9*, 263–265. (In Chinese) [CrossRef]
22. Nemes, A.; Schaap, M.; Leij, F. *The UNSODA Unsaturated Soil Hydraulic Database Version 2.0*; US Salinity Laboratory: Riverside, CA, USA, 1999.
23. Tinjum, J.M.; Benson, C.H.; Blotz, L.R. Soil-water characteristic curves for compacted clays. *J. Geotech. Geoenviron. Eng.* **1997**, *123*, 1060–1069. [CrossRef]
24. Zhu, X. Research on the Relationship between Fractal Characteristics of Soil Particle Size and Hydraulic Properties for Unsaturated Soils. Master's Thesis, Hubei University of Technology, Wuhan, China, 2019. (In Chinese).
25. Fredlund, M. *Soilvision 2.0, a Knowledge-Based Database System for Unsaturatedsaturated Soil Properties, Version 2.0*; Soilvision Systems Ltd.: Saskatoon, SK, Canada.